Research Article

Hippocampal ERK2 dimerization is critical for memory reconsolidation and synaptic plasticity

Santiago Ojea Ramos[1], Candela Medina[1,2,3], María del Carmen Krawczyk[2,3*], Julieta Millan[3*], María Florencia Acutain[4*], Arturo Gabriel Romano[1,2], María Verónica Baez[4], Francisco José Urbano[1,2], Mariano Martín Boccia[3], Mariana Feld[1#]

[1] Instituto de Fisiología, Biología Molecular y Neurociencias (IFIBYNE), Universidad de Buenos Aires (UBA) – Consejo Nacional de Investigaciones Científicas y Técnicas (CONICET).

[2] Departamento de Fisiología, Biología Molecular y Celular "Prof. Héctor Maldonado", Facultad de Ciencias Exactas y Naturales, UBA.

[3] Laboratorio de Neurofarmacología de Procesos de Memoria, Cátedra de Farmacología, Facultad de Farmacia y Bioquímica – UBA.

[4] Instituto de Biología Celular y Neurociencias "Prof. Dr. E. de Robertis" (IBCN), CONICET - UBA.

[#]**Corresponding author**: Mariana Feld, Email: mfeld@fbmc.fcen.uba.ar.

*These authors contributed equally to this work.

ABSTRACT

Extensive research has focused on extracellular-signal regulated kinase (ERK) 1/2 phosphorylation across various memory and plasticity models. However, the precise mechanism linking ERK activity to memory stabilization and restabilization are still poorly understood, and the role of ERK1/2 dimerization remains unexplored. ERK dimerization is essential for the binding and activation of cytoplasmic targets, many of which have been strongly implicated in memory and plasticity. In this work, we studied the role of ERK2 dimerization in memory and synaptic plasticity through several experimental approaches. We found that reactivation of a weak inhibitory avoidance (wIA) memory led to a significant reduction in hippocampal ERK2 dimerization. Furthermore, intrahippocampal infusion of DEL-22379 (DEL), an ERK dimerization inhibitor, following memory reactivation had a bidirectional effect: it blocked the reconsolidation of a strong inhibitory avoidance (sIA) memory, but enhanced the reconsolidation of a wIA memory. Moreover, DEL administration blocked hippocampal ERK2 dimerization in vivo and impaired high-frequency stimulation-induced long-term potentiation (LTP) in hippocampal slices. These findings demonstrate for the first time that ERK2 dimerization occurs in the intact rodent nervous system and plays a pivotal role in plasticity and memory. While further research is needed, this study highlights the relevance of ERK dimerization in these processes.

Keywords

Mice, DEL-22379, Memory reconsolidation, hippocampus, LTP, EGF

Abbreviations

ERK1/2	extracellular signal-regulated kinase 1/2
IA	Inhibitory avoidance
LTM	long-term memory
LTP	long-term potentiation
wIA	weak Inhibitory Avoidance
sIA	strong Inhibitory Avoidance
PFA	paraformaldehyde
RE	memory reactivated animals
NR	non-reactivated animals
EGF	epidermal growth factor
DEL	DEL-22379
Veh	Vehicle
DMSO	dimethyl sulfoxide
IQR	Interquartile range
TR	training
RE	memory reactivated animals
TS	testing

INTRODUCTION

The molecular mechanisms underlying learning and memory have been extensively studied in the last decades using diverse experimental paradigms and techniques. Long-term plasticity is widely considered the cellular correlate of memory formation (Bliss and Collingridge, 1993; Bliss and Lømo, 1973). In line with this proposal, specific signaling pathways, such as extracellular signal-regulated kinase 1/2 (ERK1/2) have been implicated in both plasticity and memory processes (Atkins et al., 1998; Blum et al., 1999; English and Sweatt, 1997; Martin et al., 1997; Schafe et al., 2000; Walz et al., 1999). Pharmacological inhibition of ERK1/2 phosphorylation impairs both memory formation and neuronal plasticity (reviewed in Ojea Ramos et al., 2022).

ERK1/2 belongs to the mitogen-activated protein kinase (MAPK) family, a large group of Ser/Thr protein kinases originally associated with development, mitogenesis, and stress response (Lavoie et al., 2020). ERK activation is achieved through dual phosphorylation of residues Thr and Tyr in a common TEY motif (pERK hereafter) by a MAPK/ERK kinase (MEK), inducing conformational changes that lead to substrate binding and phosphorylation. While ERK phosphorylation was initially thought to drive dimerization and subsequent nuclear translocation (Khokhlatchev et al., 1998), subsequent findings revealed that dimerization primarily mediates extra-nuclear function, enabling the activation of cytoplasmic targets via scaffolding proteins (Casar et al., 2008). Inhibition of ERK1/2 dimerization selectively impairs cytoplasmic signaling without disrupting phosphorylation (Herrero et al., 2015). Furthermore, the multiplicity of ERK1/2 cytosolic targets (Ahn, 2009; Earnest et al., 1996; Gong and Tang, 2006; Kelleher et al., 2004; Kneussel and Wagner, 2013; Schrader et al., 2006) supports the idea that extra-nuclear localization of the kinase is relevant for a wide variety of processes. DEL-22379 (DEL), a novel ERK dimerization inhibitor, effectively blocks hyperactive Ras-ERK1/2 signaling in tumor cells, impairing proliferation and transformation while circumventing resistance mechanisms previously described for phosphorylation inhibitors (Herrero et al., 2015). While oncological research has significantly advanced our understanding of ERK's role in cellular function, neuronal activation of this pathway likely exhibits distinct characteristics due to differences in subcellular localization and kinetics, particularly in processes such as synaptic plasticity, learning and memory.

In neuronal systems, ERK phosphorylation has been observed at pre- and post-synaptic sites of pyramidal neurons of the visual cortex following visual stimulation, with a temporal profile similar to cell body activation (Boggio et al., 2007). High-frequency stimulation induced ERK activation at active synapses in the medial perforant pathway, regulating translation within specific subcellular compartments (Pirbhoy et al., 2017). Additionally, NR2A-mediated ERK activation has been shown to modulate dendritic spine density in key brain areas involved in cognition (Gao et al., 2011) and has also been implicated in neurodegenerative pathologies, depending on developmental stage, cell type, and anatomical structure (Albert-Gascó et al., 2020).

Stability of consolidated memories can be challenged by reactivation, opening a new period of sensitivity named “reconsolidation” and triggering molecular mechanisms involved in re-stabilization (Dudai and Eisenberg, 2004; Nader et al., 2000; Sara, 2000). Previous work from our group demonstrated that cytosolic ERK activation is essential for the consolidation and reconsolidation of memories in invertebrates (Feld et al., 2005) and vertebrates (Krawczyk et

al., 2016, 2015). In mice, cytosolic ERK kinetics following inhibitory avoidance memory reactivation in mice regulate the reconsolidation, strength and persistence of the memory (Krawczyk et al., 2019, 2016, 2015). Additionally, nuclear ERK overactivation has been linked to memory impairment in a mouse model of Alzheimer's disease, in which partial inhibition has been shown to restore memory retention (Feld et al., 2014). These findings underscore the importance of compartment-specific ERK activation in memory processes, though critical aspects remain mostly unexplored in literature.

While ERK1/2 phosphorylation has been extensively studied, the role of ERK1/2 dimerization in synaptic plasticity and memory remains unknown. We hypothesized that ERK dimerization is a regulatory milestone for long-term memory (LTM) reconsolidation. Here we show for the first time that ERK2 dimerization can be pharmacologically inhibited in mice hippocampi without affecting its phosphorylation. DEL administration blocked CA1 hippocampal LTP and affected memory reconsolidation of the inhibitory avoidance (IA) task, with effects depending on the training strength. These findings reveal a previously unrecognized role of ERK dimerization *in vivo* in the nervous system, emphasizing its importance in synaptic plasticity and memory.

RESULTS

ERK dimerization in the rodent nervous system and plasticity

The latency to enter the dark compartment in the inhibitory avoidance (IA) task partially depends on the intensity of the aversive stimulus delivered during training (Krawczyk et al., 2019). Previous work from our group showed that retrieval of a consolidated IA memory in CF-1 mice modulated hippocampal cytosolic phosphorylated ERK2 (pERK2) levels 45 min later, depending on the strength of the training stimulus. Thus, weak IA (wIA) memory reactivation significantly increased pERK2 levels compared to naïve animals, while strong IA (sIA) memory reactivation led to a significant decrease. Furthermore, intrahippocampal administration of the MEK1/2 inhibitor PD098059, 45 min after wIA retrieval strengthened memory when tested 24 h later (Krawczyk et al., 2015).

Given the importance of cytosolic ERK activity in memory reconsolidation and the role of dimerization in regulating ERK subcellular signaling (Casar et al., 2008), we investigated whether ERK dimerization influences IA memory stabilization after reactivation. The small molecule DEL-22379 (DEL) has been shown to inhibit ERK dimerization without affecting its phosphorylation, and with no apparent toxicity (Herrero et al., 2015; Zaballos et al., 2022). However, ERK dimerization has not yet been characterized in the nervous system.

Consequently, our first experiment aimed to study ERK2 dimerization in the rodent brain (fig. 1). To induce ERK2 dimerization, two protocols were used: 1) chemical LTP (cLTP) induced in rat primary neuronal cultures using glycine stimulation (Swanger et al., 2013) and 2) intrahippocampal stimulation with EGF, an ERK1/2 pathway activator that also induces its dimerization (Casar et al., 2008). Next, protein-enriched samples were resolved in native polyacrylamide gels and transferred to nitrocellulose membranes. Initial assessment in HEK-293T cell cultures showed an increase of ERK2 dimerization after EGF stimulation (fig. 1A) consistent with previous results (Herrero et al., 2015). Furthermore, glycine-induced cLTP also upregulated ERK2 dimerization, which was abolished by 30 min-incubation with DEL (fig. 1A). These findings show that ERK dimerization occurs in primary neuronal cultures.

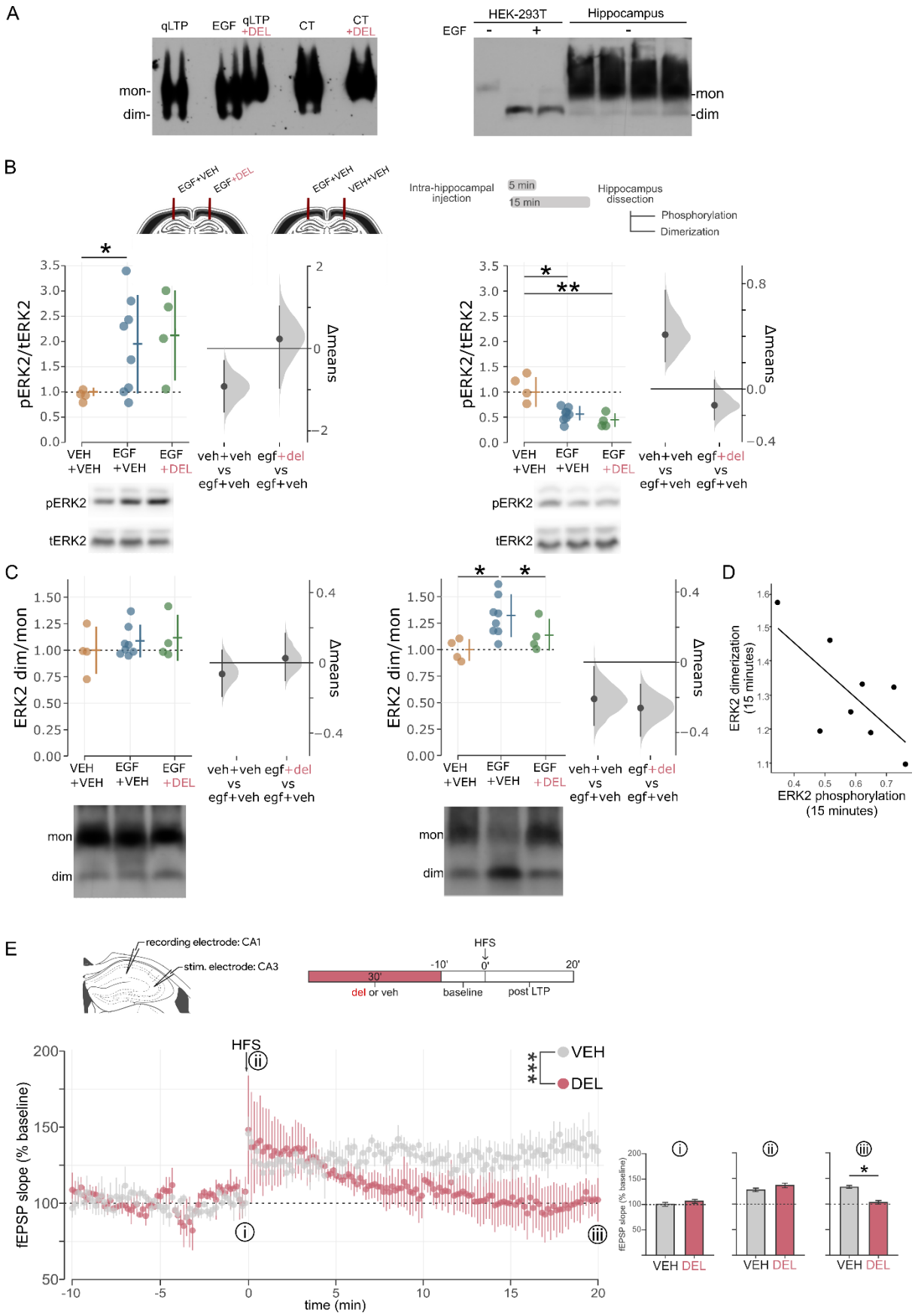

Figure 1. In vivo ERK2 dimerization in the rodent nervous system. **A)** Native PAGE western blot showing ERK2 dimers (dim) and monomers (mon) in samples from rat neuronal primary cultures subjected to either cLTP or EGF

stimulation and-or DEL treatment (left). Control and EGF-stimulated HEK-293T culture cells and CF-1 mice hippocampal protein homogenates (right). **B-C)** ERK2 phosphorylation precedes dimerization in EGF-stimulated CF-1 mice hippocampal tissue (schematic experimental design is shown on top of fig. B; representative western blot images are shown below each graph). Hippocampal ERK2 phosphorylation **(B)** and dimerization **(C)** were assessed 5 (left) or 15 (right) min after *in vivo* local EGF plus VEH or DEL administration. Dimer / monomer (dim/mon) ratios were normalized against "veh + veh" mean value in each case. Circles represent individual mice measurements, single lines represent mean ± s.d., and estimation plots shown on the right of each graph represent the difference between means (black dot) and the bootstrapped distribution of means (grey area) with 95% confidence intervals. *****, $p < 0.05$; ******, $p < 0.01$ in Tukey comparisons. n = 4 mice / group. **D)** Pearson correlation between ERK2 phosphorylation and dimerization assessed at 15 min in figures B and C. $R^2 = 0.71$; $p < 0.05$. **E)** DEL pre-treatment impairs LTP in CA1 hippocampal acute slices (schematic stimulation/recording sites and experimental design is shown on top). Circles represent the mean of 4 replicates and single lines represent s.d. Three points of interest are indicated throughout the recording: immediately before stimulation (i), immediately after stimulation (ii), and approx. 18-20 min after stimulation (iii). Bars in i), ii) and iii) are the mean ± s.d. of 100 sec recordings. ***, $p < 0.05$ (repeated measures comparison between VEH- and DEL-treated groups). n = 4 mice / group.

Since primary neuronal cultures lack the physiological tissue context of the hippocampus, we next evaluated ERK2 dimerization *in vivo*. In the second experiment, we assessed the efficacy of DEL to inhibit ERK2 dimerization in CF-1 mice hippocampus. We acutely injected either PBS (VEH) or EGF plus either VEH or DEL in each hemi-hippocampus of CF-1 anesthetized mice. Afterwards, mice were euthanized, and we performed SDS and native gel electrophoresis of protein-enriched hippocampal samples and western blot. A schematic experimental design is shown on top of figure 1B. This administration scheme was used to perform experimental and control treatments in the same animal. Consistent with previous reports (Marshall, 1995; Nguyen et al., 1993; Traverse et al., 1992; Xing and Imagawa, 1999), EGF administration altered hippocampal pERK2 levels 5 (fig. 1B left; $F_{2,13} = 5.381$, $p = 0.048$) and 15 min later (fig. 1B right; $F_{2,13} = 8.582$, $p = 0.010$). EGF administration induced a rapid and transient significant increase in hippocampal pERK2 at 5 min ($p = 0.049$) which decreased under VEH baseline levels at 15 min ($p = 0.010$). It is important to point out that DEL treatment did not affect EGF-induced pERK2 at the time points assessed ($p = 0.989$ at 5 min; $p = 0.555$ at 15 min in EGF-VEH vs EGF-DEL contrasts), which were also statistically different from control ($p = 0.036$ at 5 min; $p = 0.009$ at 15 min in VEH-VEH vs DEL-EGF contrasts). However, ERK2 dimerization (fig. 1C) showed a distinct time course after EGF administration: it did not change at 5 min (fig. 1C left; $F_{2,13} = 0.270$; $p = 0.769$), but significantly increased at 15 min (fig. 1C right; $F_{2,13} = 11.623$; $p = 0.004$). Consistent with previous results (Herrero et al., 2015), EGF alone induced a significant rise in ERK2 dimerization ($p = 0.014$). This effect was prevented by DEL administration ($p = 0.030$) which induced dimer/monomer (dim/mon) levels comparable to VEH-treated controls ($p = 0.915$). Furthermore, phosphorylation and dimerization of ERK2 showed a strong negative correlation 15 min after stimulation (fig. 1D, $p = 0.049$). Thus, based on these findings, under our experimental conditions DEL prevents ERK2 dimerization induced by EGF in CF-1 mice hippocampi without affecting its phosphorylation.

To assess whether the inhibition of ERK2 dimerization has an impact on hippocampal plasticity we performed LTP experiments on hippocampal slices. Slices were pre-incubated for 30 min with DEL or VEH and after drug washout baseline field excitatory post-synaptic potentials (fEPSP) were recorded for 10 min, followed by high frequency stimulation (HFS) on Schaffer Collaterals (5 trains, 100 Hz, 10 pulses). While HFS was able to induce LTP in the CA1 in both DEL and VEH treated slices (mean ± standard deviation of fEPSP slope relative to the baseline immediately post-HFS: VEH = 1.45 ± 0.12, DEL = 1.47 ± 0.16, $p = 0.058$), suggesting that

ERK dimerization is not necessary for LTP induction, fEPSPs slope in DEL-treated slices returned to baseline levels (fEPSPs slope 20 minutes after HFS: VEH = 1.34 ± 0.21, DEL = 1.02 ± 0.20, p = 0.022), indicating that inhibiting ERK dimerization prevents the maintenance of CA1 LTP induced by HFS.

These results demonstrate that DEL selectively inhibits ERK2 dimerization in the mouse hippocampus without affecting its phosphorylation and suggest that dimerization plays a critical role in hippocampal synaptic plasticity.

Memory reactivation after Weak IA decreases hippocampal ERK dimerization

Since ERK dimerization can modulate hippocampal plasticity, and that IA memory reconsolidation is fine-tuned by cytoplasmic ERK signaling 45 min after reactivation (Krawczyk et al., 2015), we investigated whether hippocampal ERK dimerization is regulated by memory reactivation at this time point. Animals were trained using either strong (sIA) or weak (wIA) versions of the IA task and subjected to memory reactivation (RE) 48 hours later. Identically trained animals not exposed to reactivation (NR) served as controls. Animals were euthanized 45 min after reactivation (RE groups) or the corresponding time point (NR groups), and ERK2 dimerization was assessed in hippocampal protein samples electrophoresed in native polyacrylamide gels (fig. 2, scheme).

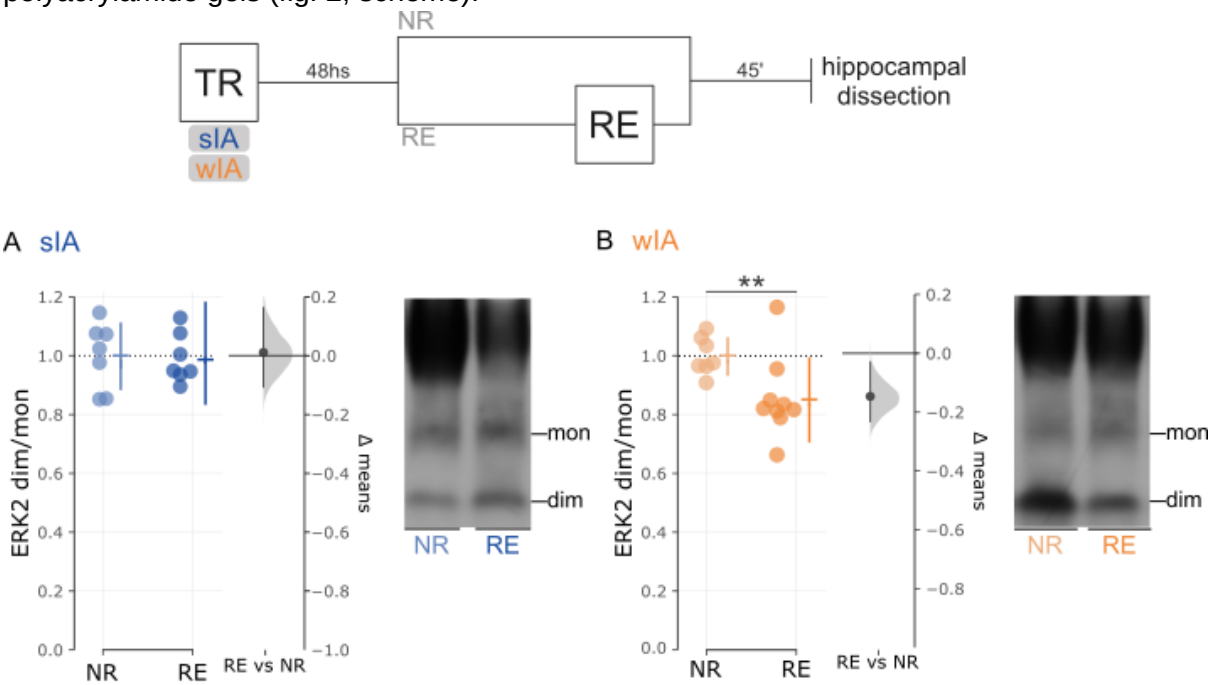

Figure 2. Hippocampal ERK2 dimerization after memory reactivation. **Top)** Schematic experimental design for ERK2 dimerization assessment. **Bottom)** Hippocampal ERK2 dimerization assessment by native PAGE western blots 45 after either sIA **(A)** or wIA **(B)** memory reactivation. Dim/mon ratios are normalized against NR mean value for each experiment. Color circles indicate individual values and error bars shown on the right of each set depict mean ± s.d. values. Estimation plots shown on the right of each graph represent the difference between means (black dot) and the bootstrapped distribution of means (grey area) with 95% confidence intervals. Representative western blots are also shown (right). *****, p < 0.05; ******, p < 0.01 in Tukey comparisons. n = 7-9 / group.

Reexposure to the IA context 48 hours after sIA did not induce significant changes in hippocampal ERK2 dimerization relative to NR controls 45 minutes post-reactivation (fig. 2A;

t_{13} = 0.161; p = 0.873). In contrast, wIA memory reactivation led to a significant decrease in ERK2 dimerization compared to the NR control group (fig. 2B; t_{14} = 2.569; p = 0.022).

The finding that memory reactivation induced differential ERK2 dimerization depending on training strength suggests the possibility that this molecular mechanism plays a role in memory reconsolidation.

Post-retrieval hippocampal ERK2 dimerization supports strong IA memories

Given the differential regulation of ERK2 dimerization after memory reactivation, we next investigated whether its inhibition would affect memory reconsolidation, a process triggered by reactivation. First, we assessed whether intrahippocampal DEL administration after memory reactivation altered ERK2 dimerization levels. For this experiment, animals were injected with either VEH or DEL in both hippocampi 35 minutes either after RE or the corresponding time for NR animals (fig. 3A, upper scheme). Ten minutes later, animals were euthanized, and their hippocampi were removed and homogenized. As shown in figure 3A (lower panel), memory reactivation alone did not induce changes in ERK2 dimerization levels ($F_{2,21}$ = 5.559; p = 0.012; p = 0.336 in NR-VEH vs RE-VEH contrast). However, hippocampal DEL injection after reactivation significantly reduced ERK2 dimerization (p = 0.010 in RE-DEL vs NR-VEH contrast), mimicking the reduction observed following wIA reactivation.

To determine whether basal ERK2 dimerization levels are necessary for strong IA memory reconsolidation, we administered either VEH or DEL 40 min after strong IA memory reactivation and tested retention 24 hours later (fig. 3B, upper panel). During training and reactivation all groups performed similarly, and reactivated groups exhibited robust retention during context reexposure (fig. 3B, lower panel). However, there was a significant interaction between reactivation and drug treatment on latencies during the test session ($F_{2,28}$= 5.291; p = 0.029). Specifically, DEL-treated RE-animals showed significantly reduced latencies compared to the VEH-treated ones (p = 0.029), while latencies from VEH- and DEL-injected NR group were not statistically different (p = 0.983). Furthermore, latencies from VEH-injected groups were consistent across conditions (p = 0.685). This impairment was sustained for at least a week (suppl. fig. 1), suggesting a specific effect on the reconsolidation process.

Together, these findings indicate that basal ERK2 dimerization is critical for the reconsolidation of sIA memories.

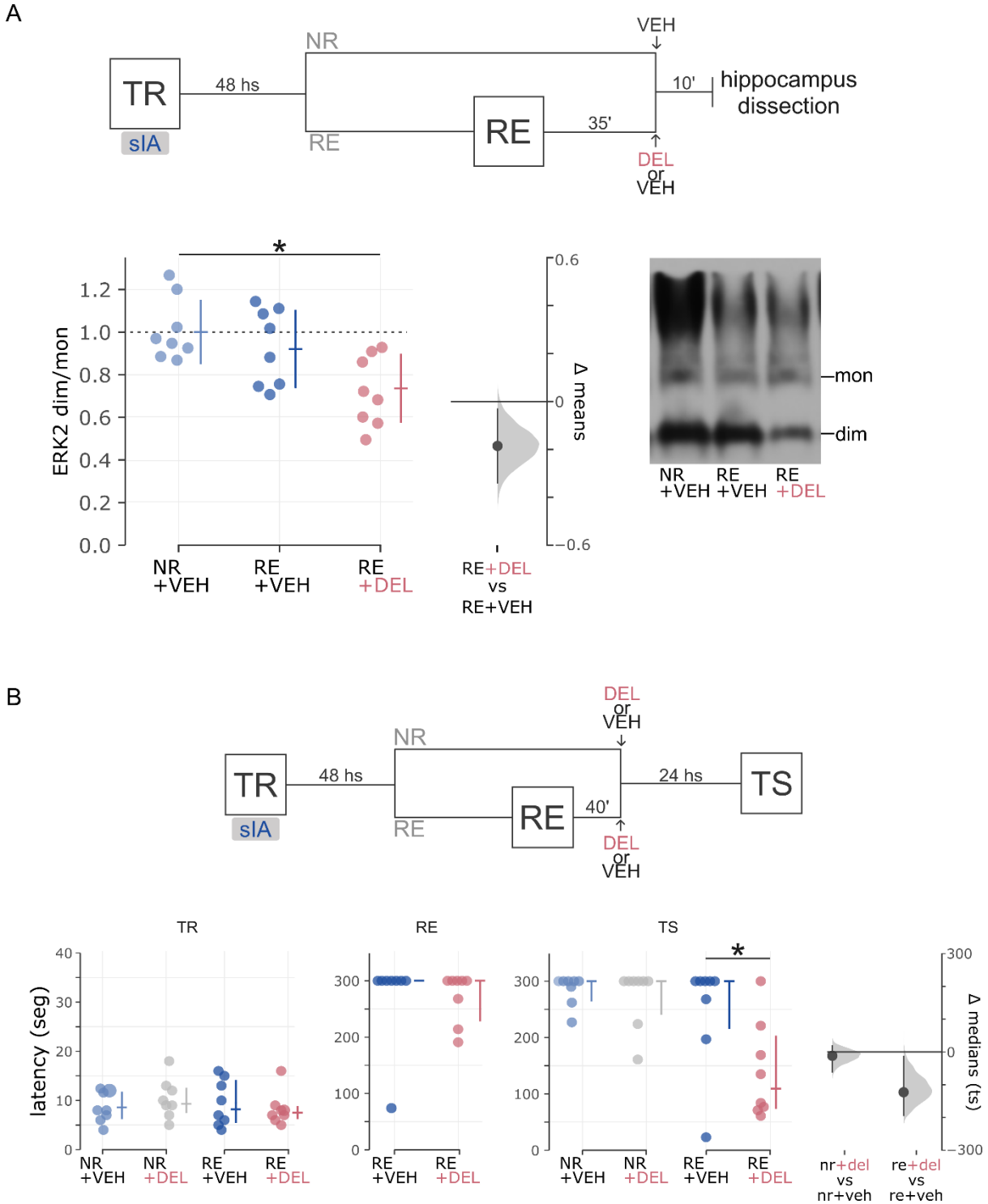

Figure 3. Role of hippocampal ERK2 dimerization after sIA memory reactivation. **A)** DEL decreases hippocampal ERK2 dimerization after sIA memory reactivation. Schematic experimental design for hippocampal ERK2 dimerization assessment is shown **(top)**. Hippocampal ERK2 dimerization was assessed 45 min after sIA memory reactivation and 10 min after VEH or DEL intra-hippocampal administration. Dimer to monomer ratios were normalized against NR mean value for each experiment. Color circles indicate individual values and error bars shown on the right of each dataset depict mean ± s.d. values. Estimation plot on the right represents the difference between means (black dot) and the bootstrapped distribution of means (grey area) with 95% confidence intervals. Representative western blots are also shown (right). *****, $p < 0.05$; ******, $p < 0.01$ in Tukey adjusted *post hoc* comparisons. n = 8 / group. **B)** Inhibition of hippocampal ERK2 dimerization after strong IA memory reactivation

impairs LTM. Schematic experimental design is shown **(top)**. Color circles indicate individual latencies to step through values and error bars shown on the right of each set depict median ± inter quartile range (IQR). Estimation plot on the right of TS graph represents the difference between means (black dot) and the bootstrapped distribution of means (grey area) with 95% confidence intervals. *****, $p < 0.05$; ******, $p < 0.01$ in Tukey adjusted *post hoc* comparisons. n = 8 / group.

Inhibiting hippocampal ERK dimerization after reactivation strengthens weak IA memories

Given that wIA memory reactivation decreased ERK2 dimerization in mice hippocampi (fig. 2B), we next investigated whether inhibiting ERK2 dimerization after wIA reactivation would influence memory reconsolidation. To evaluate this, we trained four groups of animals in a wIA task and submitted two of them to memory reactivation (RE) 48 hours later. Performance during training was consistent across all groups. As expected, RE groups expressed median latencies of ≈150 seconds during the reactivation. One NR and one RE group of animals were administered VEH, while the remaining NR and RE groups were injected DEL in the dorsal hippocampus 40 min after the reactivation session (fig. 4A). Testing 24 hours later revealed a significant interaction between reactivation and drug treatment ($F_{2,30} = 13.254$; $p = 0.001$). Remarkably, DEL-treated RE-animals showed significantly higher latencies than the VEH-treated ones ($p = 0.005$). This enhancement was specific to reactivated groups, as NR animals did not show significant differences in latencies between VEH and DEL treatment during test ($p = 0.379$). Furthermore, VEH-treated groups did not differ statistically in their latencies during the test session ($p = 0.273$).

Not only did DEL administration improve retention in reactivated animals, but it also increased the proportion of animals with higher latencies during the test session compared to reactivation (suppl. fig.2). A significant positive correlation was observed between RE and TS response levels in DEL-RE animals (suppl. fig. 2; $R^2 = 0.73$; $p = 0.025$), contrasting with the VEH-RE group (suppl. fig. 2; $R^2 = 0.42$; $p = 0.270$).

Finally, ERK2 dimerization levels were significantly modulated by reactivation also in VEH/DEL-injected animals as well ($F_{2,21} = 13.254$; $p = 0.0002$). In contrast to what we observed after sIA training, wIA memory reactivation led to a significant decrease in ERK2 dimerization (see fig. 2B) which was also observed after VEH-administration in mice hippocampi (fig. 4B; $p = 0.006$). However, DEL injection did not significantly affect ERK2 dimerization levels following memory reactivation ($p = 0.375$), though these levels were significantly different from those in the control group NR-VEH ($p = 0.0003$).

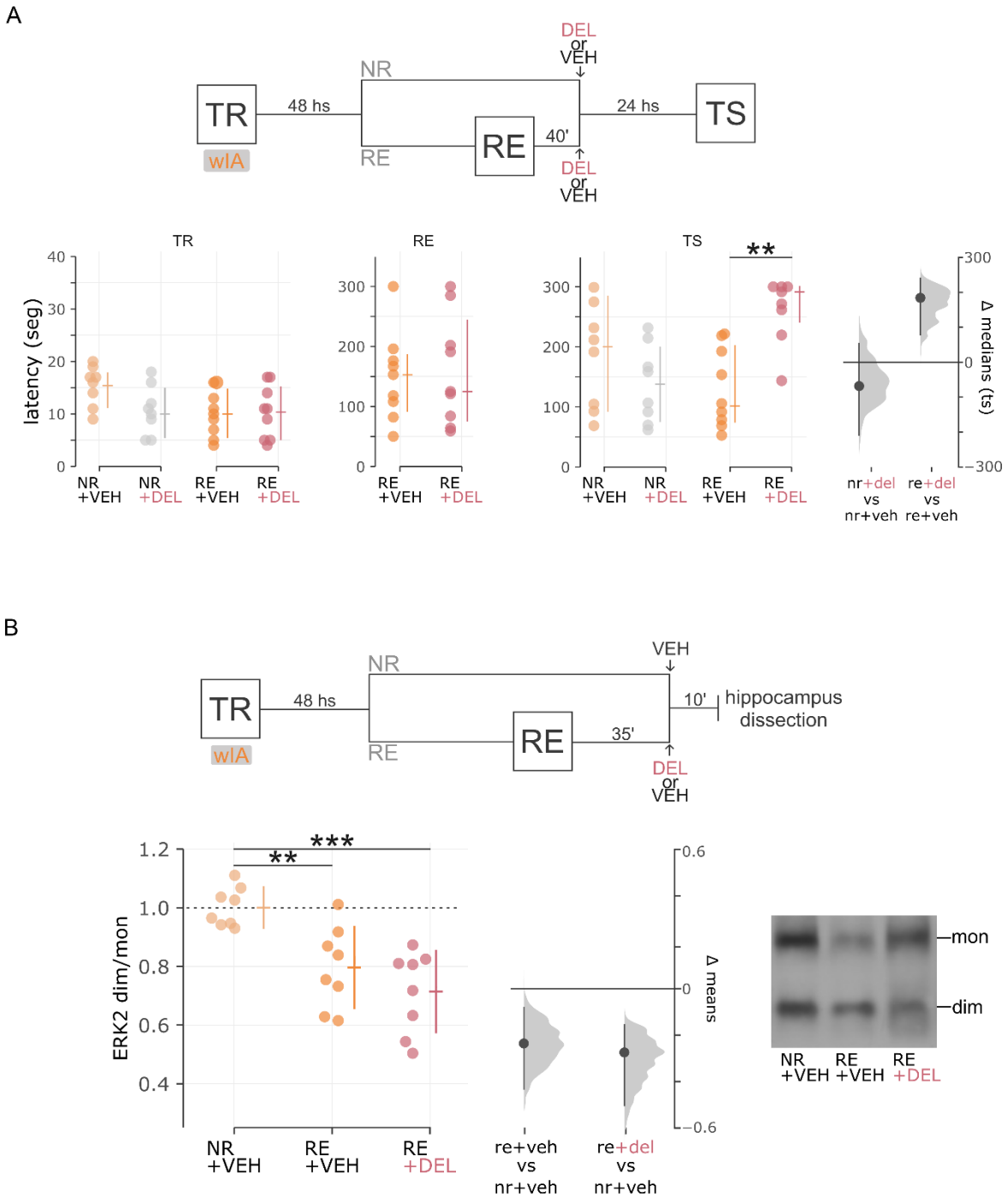

Figure 4. Role of hippocampal ERK2 dimerization after wIA memory reactivation. **A)** Inhibition of hippocampal ERK2 dimerization after strong IA memory reactivation improves LTM. Schematic experimental design is shown on top. Color circles indicate individual latencies to step through values during training (TR, left), reactivation (RE, center) and testing (TS, right). Error bars shown on the right of each dataset depict median ± IQR. Estimation plot on the right of TS graph represent the difference between means (black dot) and the bootstrapped distribution of means (grey area) with 95% confidence intervals. *****, $p < 0.05$; ******, $p < 0.01$ in Tukey adjusted *post hoc* comparisons. n = 8 - 9 / group. **B)** Hippocampal ERK2 dimerization decreases after wIA memory reactivation. Schematic experimental design is shown on top. Color circles indicate individual values and error bars shown on the right of each dataset depict mean ± s.d. values. Estimation plots on the right of the graph represent the differences between means (black dot) and the bootstrapped distribution of means (grey area) with 95% confidence intervals. Representative western blots are also shown (right). *****, $p < 0.05$; ******, $p < 0.01$ in Tukey adjusted *post hoc* comparisons. n = 8 / group.

These results demonstrate that inhibiting ERK2 dimerization after reactivation enhances retention of wIA memories, suggesting that the decrease in ERK2 dimerization associated with wIA reactivation may represent a boundary condition for memory reconsolidation that can be shifted by pharmacological intervention.

DISCUSSION

In this work, we show for the first time that ERK2 dimerization constitutes a key regulatory step in neuronal plasticity and memory processes. Several lines of evidence indicate that subcellular localization of a particular intracellular signaling pathway activity is crucial for specific biological outcomes (Afinanisa et al., 2021; Casar and Crespo, 2016; Formoso et al., 2020). In the central nervous system, NF-kappaB was shown to be regulated in a subcellular localization-specific manner by different memory and learning processes (Salles et al., 2015). Over the past decade, oncological research has advanced the development of drugs targeting key pathways to reverse pathological conditions. Interestingly, many of these pathways have also been implicated in learning and memory processes. However, their regulatory mechanisms within the nervous system often remain poorly understood. ERK signaling serves as a notable example. ERK phosphorylation is well known to be essential for neural plasticity and cognitive processes, and its deregulation often leads to pathological conditions (reviewed in Ojea Ramos et al., 2022). Interestingly, ERK dimerization has been proposed to regulate the subcellular location of its activity, thereby influencing the phosphorylation of specific targets and ultimately the cellular fate (Casar and Crespo, 2016; Herrero et al., 2015). However, despite extensive studies on neural ERK activation, the functional role of ERK dimerization in the nervous system remains largely unexplored.

Consequently, we first established that ERK dimerization occurs in neural tissue, both *in vitro* using primary neuronal cultures and *in vivo* within the hippocampus of CF-1 mice. Primary neuronal cultures stimulated with either EGF or a glycine-based cLTP protocol increased ERK2 dimerization, an effect that was inhibited by DEL pre-treatment (fig. 1A). Similarly, *in vivo* EGF stimulation induced hippocampal ERK2 dimerization, which was prevented by DEL treatment without affecting ERK phosphorylation (fig. 1B and 1C). This findings align with previous studies in cancer cells showing that EGF stimulation induces ERK dimerization (Herrero et al., 2015). In physiological contexts, EGF concentration plays a critical role in determining cellular responses, with variations influencing the balance between migratory and proliferative states (Brüggemann et al., 2021). At low concentrations—typical of paracrine signaling during early wound closure—EGF fails to elicit robust proliferative ERK signaling in the cytoplasm. Instead, it promotes pro-migratory signaling by activating KSR-ERK complexes at the plasma membrane, thereby enhancing cell migration (Brüggemann et al., 2021). The EGF concentration used in our culture experiments was consistent with that employed by Herrero et al. (2015) in HEK293T cells and with doses known to promote proliferation in MCF7 cells (Brüggemann et al., 2021). To validate our findings, we replicated the experiments conducted by Herrero and colleagues, using them as a reference to evaluate ERK2 dimerization in rodent neural tissue (fig. 1A). EGF has been shown to induce rapid and transient ERK phosphorylation in PC12 cells, a process linked to cell proliferation (Traverse et al., 1992), and we observed similar kinetics in our study. Like many other tissues, the brain expresses EGF receptors, which regulate neurite outgrowth and neuronal homeostasis (Romano and Bucci, 2020). However, distinct ligands can induce different ERK activation kinetics and cellular outcomes (Miningou and Blackwell, 2020). Recent research on breast

tumors has demonstrated that ligand-dependent ERK dimerization is crucial for cellular motility as its disruption impairs actin cytoskeleton rearrangements (de la Fuente-Vivas et al., 2024). How ERK dimerization is modulated by ligand specificity and its functional consequences in neurons remain open questions for future investigation.

ERK dimerization in plasticity

Hippocampal plasticity has been proposed as a cellular correlate of experience-coding leading to memory formation and storage. Since the seminal work by English and Sweatt (1997), which demonstrated that ERK inhibition blocks HFS-induced LTP in the CA1 region of rat hippocampus, multiple studies have provided evidence supporting its role in these processes (Atkins et al., 1998; Impey et al., 1998; Kelleher et al., 2004; Selcher et al., 2003, reviewed in Ojea Ramos et al., 2022). A key finding in this field is that HFS protocol applied to the Schaffer Collaterals induces ERK2 phosphorylation in the CA1 region of rodent brain, and that blocking ERK phosphorylation prior to LTP induction prevents its long-term maintenance (English and Sweatt, 1997).

Building on this, a plausible hypothesis is that ERK dimerization may regulate synaptic plasticity and memory processes. In our study, we found that DEL pre-treatment on acute hippocampal slices impaired long-term LTP stabilization without affecting its initial induction. Together with previous findings, our results suggest that both ERK phosphorylation and dimerization are crucial for LTP maintenance. Moreover, ERK phosphorylation and dimerization have been shown to compartmentalize signaling within specific subcellular regions (Casar and Crespo, 2016). Thus, dimerization may spatially regulate distinct ERK signaling pools that differentially contribute to plasticity and memory. Since ERK dimerization and phosphorylation target different neuronal compartments, it is likely that at least two distinct pathways are triggered during ERK signaling. Moreover, memory processes involve the activation of multiple receptor systems, which, in turn, engage various molecular pathways that influence ERK signaling, ultimately shaping its kinetics and downstream effects. Consequently, it is plausible that ERK2 dimerization also plays a role in LTP induction, yet the precise dynamics of its involvement in this process remain an open question.

ERK dimerization in inhibitory avoidance memory reconsolidation

To this day, ERK signaling has been considered a key pathway for LTM consolidation (Atkins et al., 1998; Blum et al., 1999; Feld et al., 2005; Schafe et al., 2000; Selcher et al., 2003; Walz et al., 1999). It has also been proposed as one of the molecules involved in memory labilization and reconsolidation, becoming activated in the same set of neurons previously engaged during conditioning upon memory reactivation (Zamorano et al., 2018). It is worth noting that ERK's role in plasticity and memory processes has been attributed almost exclusively to phosphorylation, leaving the potential involvement of other post-translational modifications in regulating these processes largely unexplored.

Our results reveal a dual role for ERK2 dimerization in inhibitory avoidance (IA) memory reconsolidation, depending on the strength of the stimuli used in the training session. After strong IA (sIA) training, intra-hippocampal DEL administration impaired memory reconsolidation, while after weak IA (wIA) the same manipulation enhanced memory retention. These findings suggest that the molecular mechanisms engaged upon memory reactivation are dependent on training conditions, with hippocampal ERK dimerization playing opposite

roles in the behavioral outcome of sIA and wIA reconsolidation. Notably, it has been reported that pharmacological inhibition of ERK dimerization increases its nuclear signaling (Casar et al., 2008). In this line, sIA and wIA may engage different spatial ERK pools that could explain the bidirectional effect observed. Moreover, distinct pool-specific components (e.g. upstream ligands and/or downstream targets) of the ERK pathway may guide different cellular fates. For instance, a strong stimulus could trigger protein translation via ERK activation and promote gene transcription via ERK nuclear translocation. In this scenario, ERK inhibition would impair memory by disrupting these mechanisms. Conversely, after a weak stimulus, DEL might enhance memory by promoting protein synthesis through alternative pathways. This could compensate for reduced ERK activation and facilitate memory reconsolidation. On the other hand, the possibility that sIA and wIA memory reactivation might recruit distinct neural circuits within the hippocampus cannot be discarded. Supporting these hypotheses, it was observed that protein synthesis inhibition after reactivation exerted differential effects on memory restabilization of an IA task in mice according to the area infused. In that work, protein synthesis immediately after reactivation was required in the amygdala in order to support memory reconsolidation while in the hippocampus and mPFC it was necessary to enhance retention independent from retrieval (Fukushima et al., 2014). Further experiments will be needed to elucidate how inhibiting ERK dimerization exerts a bidirectional effect on memory reconsolidation, depending on the strength of the training stimuli.

Our experiments also confirmed that the effect on hippocampal ERK dimerization is specific to the reconsolidation process, as non-reactivated (NR) animals did not show changes in step through latency following DEL treatment (figures 3B and 4A). Furthermore, sIA reconsolidation memory impairment following DEL administration persisted for at least one week (suppl. fig. 1), suggesting that there was no spontaneous recovery of the original memory, which would have suggested the possibility of the enhancement of an extinction process.

In the present manuscript, we showed for the first time evidence of ERK2 dimerization playing a critical regulatory role in the central nervous system. Our findings reveal that ERK2 dimerization is essential for hippocampal plasticity and memory reconsolidation, introducing a novel mechanism of ERK2 regulation in the brain. Future studies will likely elucidate the other molecular players recruited by this mechanism.

MATERIALS AND METHODS

Animals

Different cohorts of CF-1 male mice aged either 5 weeks (weight range: 21 - 31 g, housed in groups of 3-5 individuals in 18.41 x 29.21 x 12.7 cm amber polysulfone cages at the Facultad de Ciencias Exactas y Naturales´ central animal facility) or 8-10 weeks old (weight range: 25 - 35 g, housed in groups of 18 - 22 individuals in stainless-steel 50 x 30 x 15 cm cages kept at the Laboratorio de Neurofarmacología de Procesos de Memoria, Facultad de Farmacia y Bioquímica) were used either for electrophysiological experiments or behavioral testing and biochemical analyses, respectively. The mice had *ad libitum* access to dry food and tap water and were maintained under a 12h light/dark cycle (lights on at 6:00 AM) at a controlled temperature of 21-23ºC. Experiments were conducted during the light cycle. All procedures related to care and treatments of mice were approved by the local institutional animal care and use committees (CICUAL - CUDAP # 0044975-2016, Facultad de Farmacia y Bioquímica; CICUAL # 154b, Facultad de Ciencias Exactas y Naturales, Universidad de Buenos Aires, Argentina), and in compliance with the standard European Union and United States National

Institutes of Health ethical guidelines for Care and Use of Laboratory Animals. All efforts were made to minimize any possible distress or suffering experienced by mice, as well as to reduce the number of animals required to generate reliable scientific data.

Drugs

DEL-22379 (DEL), an ERK dimerization inhibitor (Herrero et al., 2015), was purchased from MedChemExpress (Cat. No.: HY-18932) and dissolved in dimethyl sulfoxide (DMSO) as vehicle (VEH). For behavioral experiments and hippocampal ERK2 dimerization assays, 0.5 µl of drug or VEH solution were injected per hemi-hippocampus (DEL final concentration: 400 nM). Epidermal growth-factor (EGF) was purchased from Thermo Fisher (Cat. No.: PHG0314) and diluted in sterile PBS to a final concentration of 100 µM and 0.5 uL were injected per hemi-hippocampus.

Hippocampal slices and extracellular field potential recordings

Electrophysiological recordings in slices were performed as described elsewhere (Rivero-Echeto et al., 2021). Briefly, mice were deeply anesthetized with a mix of ketamine (160 mg/kg) and xylazine (8 mg/kg) before decapitation. Coronal brain slices including dorsal hippocampus (300-400 µm thick) were obtained by gluing the brain onto a vibratome stage (PELCO, EasiSlicer, Ted Pella Inc., CA, USA), submerged in a chamber containing chilled low-sodium/high-sucrose solution (250 mM sucrose, 2.5 mM KCl, 3 mM $MgSO_4$, 0.1 mM $CaCl_2$, 1.25 mM NaH_2PO_4, 0.4 mM ascorbic acid, 3 mM myo-inositol, 2 mM pyruvic acid, 25 mM D-glucose, and 25 mM $NaHCO_3$). Sequential slices were obtained in which Schaffer collaterals were transected near CA3 before being transferred to an incubation chamber and kept at 35 °C for 30 min. Recovery chamber was containing low Ca^{2+} / high Mg^{2+} normal artificial cerebrospinal fluid (ACSF; 125 mM NaCl, 2.5 mM KCl, 3 mM $MgSO_4$, 0.1 mM $CaCl_2$, 1.25 mM NaH_2PO_4, 0.4 mM ascorbic acid, 3 mM myo-inositol, 2 mM pyruvic acid, 25 mM d-glucose, and 25 mM $NaHCO_3$ and aerated with 95% O_2 / 5 % CO_2, pH 7.4). Slices were then transferred to the recording chamber and perfused continuously with ACSF including bicuculline (20 µM; a GABA-A antagonist).
Recording electrodes were made with borosilicate glass (2–3 MΩ), filled with ACSF + bicuculline solution and placed in the *stratum radiatum* area of the CA1 region of the hippocampus. The field excitatory postsynaptic potentials (fEPSP) were recorded as measure of local excitatory synaptic transmission in the CA1 region. The stimulating electrode was placed at the Schaffer Collateral fibers and fEPSPs were evoked by test stimuli (0.033 Hz, 0.05-0.2 ms duration) every 30 sec. LTP was induced by applying high frequency stimulation (HFS; 5 trains, 100 Hz, 10 pulses) after a recorded baseline period of 10 min. Recordings were maintained for 30 min after LTP induction. The magnitude of LTP was calculated as a percentage of the fEPSP slope value after HFS compared to baseline fEPSP mean slopes. Changes in LTP were compared in hippocampal slices incubated with either DEL (30 min., 1,33 µM) or VEH. Signals were recorded using a MultiClamp 700 amplifier commanded by pCLAMP 10.0 software (Molecular Devices, CA, USA). Data was filtered at 5 kHz, digitized, and stored for off-line analysis.

Intra-hippocampal injections

Hippocampal injections were performed under isoflurane anesthesia (induction: 3.5 %, maintenance: 1 %) using a stereotaxic apparatus (Stoelting) at the indicated time points. Surgery lasted for no more than 5 min. A small incision was made in the scalp and two holes were drilled in the skull at the following coordinates: AP: -1.90 mm from bregma, DV: -2.2 mm from the skull surface and +/-1.2 mm left and right from the midsagittal suture (Paxinos and Franklin, 2019) to bilaterally infuse the drugs. Injections were driven by an automatic pump

(MD-1020, Bioanalytical Systems, Inc.) at a rate of 0.52 µL/min through a 30-gauge stainless steel needle attached to a 5 µl Hamilton syringe with PE-10 tubing. n. The drug infusion lasted 60 sec and the needle was left in place for another 30 sec to avoid reflux. Total volume of administration was 0.5 µl (either drug or VEH solution) per hemi-hippocampus. At the end of the procedure, the incision was sutured and thoroughly disinfected. After the last testing session, animals were euthanized by cervical dislocation and brains were dissected, fixed by immersion in 4 % PFA overnight, and sectioned to verify the correct injection site placement. In all cases administration placement was confirmed in the target area (Suppl. Fig. 3).

Inhibitory Avoidance task

IA behavior was assessed using a one-trial step-through protocol, which takes advantage of mice's natural preference for dark and confined spaces (Blake et al., 2008; Boccia et al., 2004). The apparatus consists of a dark closed compartment (20 x 20 x 15 cm) with a stainless-steel grid floor and a small illuminated open platform (5 x 5 cm) attached to its entrance. During the training phase (TR), each mouse was placed on the illuminated platform and received a foot shock upon entry into the dark compartment. Two different shock intensities were used: a 0.3 mA - 3 sec shock for weak inhibitory avoidance induction (wIA) and a 0.4 mA - 3 sec shock for strong inhibitory avoidance (sIA) memory formation (Blake et al., 2014). Mice underwent two retention tests after TR. The first retention test, 48 h after TR, followed by a second retention test (TS) 24 h after T1. No shock was delivered during either test session. Previous work showed that T1 also induces memory reactivation (RE), and this process was controlled by means of a non-reactivated (NR) group (Boccia et al., 2007, 2010; Krawczyk et al., 2021, 2015). The retention tests were finished either when the mouse stepped into the dark compartment or failed to enter within 300 sec after the beginning of the test. After the retention test, mice were returned to their home cages. Step through latencies were manually registered by the experimenter using a manual chronometer.

Sample preparation and ERK analysis

Neuronal cultures. Primary neuronal cultures were obtained as described before (Acutain et al., 2021; Kaech and Banker, 2006). Briefly, Wistar embryos were obtained on embryonic day 17, both hippocampi were dissected from pups and digested with trypsin (Sigma, Sigma–Aldrich Co., St. Louis, MO, United States). Cells were plated onto poly-L-lysine (Sigma)–coated wells and incubated in neurobasal media (NB; Invitrogen, Life Technologies Corporation, Carlsbad, CA, United States) supplemented with B27 (Invitrogen) and Glutamax (Invitrogen). Cultures were maintained in complete NB (NB + B27 + Glutamax) at 37°C and with 5 % CO_2 and one third of the culture media was replaced every 2 days.
For the induction of ERK activation by EGF, 1 µl of the stock solution was diluted in 1 mL of culture medium and incubated in the culture for 5 min. Chemical LTP (cLTP) induction was achieved by a glycine stimulation based on a previously described (Swanger et al., 2013). Neuronal cultures were incubated with conditioned media containing 200 mM glycine for 3 min. Glycine solution was then removed and neurons were maintained in their media for 2 min of incubation. Control groups were incubated with conditioned media for 3 min without Glycine stimulation.
After treatment, neuronal cultures were cooled and homogenized by scraping cells in ice-cold lysis buffer (20 mM HEPES, pH 7.5, 10 mM ethylene glycol tetra-acetic acid, 40 mM glycerol 2-phosphate, 1 % (w/v) IGEPAL, 2.5 mM $MgCl_2$, 2 mM sodium orthovanadate, 1 mM dithiothreitol, 0.5 mM PMSF, 50 mM Sodium Fluoride, 1 µg/ml Pepstatin A, 10 µg/mL Leupeptin, 10 µg/mL Aprotinin) as described previously (Pinto and Crespo, 2010). Samples were centrifuged at 13000 x g for 10 min at 4 ºC, and the supernatants were collected and conserved at -20 ºC.

Hippocampal ERK activation and *tissue* protein extraction

For the induction of hippocampal ERK activation by EGF, two consecutive injections were performed in each hemi-hippocampus: first either 0.5 µl of phosphate buffer saline (VEH) or 100 µM EGF followed by 0.5 µl of either DMSO (VEH) or 400 nM DEL. At the specified time points, mice were quickly euthanized by cervical dislocation, decapitated and the hippocampi were dissected. Each hemi-hippocampi was then homogenized using a Dounce tight homogenizer and 125 µL of ice-cold lysis buffer (20 mM HEPES, pH 7.5, 10 mM ethylene glycol tetraacetic acid (EGTA), 40 mM glycerol 2-phosphate, 1 % (w/v) IGEPAL, 2.5 mM $MgCl_2$, 2 mM orthovanadate, 1 mM dithiothreitol, 0.5 mM PMSF, 50 mM Sodium Fluoride, 1 µg/ml Pepstatin A, 10 µg/mL Leupeptin, 10 µg/mL Aprotinin) by performing 8 strokes with a tight glass pestle. Samples were centrifuged at 13000 x g for 10 min at 4 ºC, and the cytosolic-enriched supernatants were collected and conserved at -20 ºC.

Native gel electrophoresis

Native polyacrylamide gel electrophoresis (PAGE) for ERK dimers detection was carried out as described previously (Pinto and Crespo, 2010). Briefly, protein levels in lysates were quantified by BCA Assay (Bio-Rad, USA) and 60 µg of protein were loaded into an 8 % bis-acrylamide gel and run for 150 min at 70 V. Then samples were transferred to a nitrocellulose membrane (General Electric, USA) overnight at 125 mA and 4 ºC.

SDS-PAGE

ERK phosphorylation levels were assessed by means of denaturing gel electrophoresis as described before (Krawczyk et al., 2015). Briefly, 20 µg of protein were loaded in a 12.5 % bis-acrylamide gel and run for 90 min at 100 V. The samples were then transferred to a PVDF membrane (Thermo Scientific, USA) overnight at 300 mA and 4 ºC and stored in TBS until probed with antibodies.

Antibodies used and detection

Initially, membranes were blocked in 4% non-fat dry milk in TBS - 0.05 % Tween-20. A full list of antibodies used, and dilutions can be found in Table 1. Primary antibodies were incubated overnight at 4 ºC and secondary antibodies were incubated for 1 h in TTBS at room temperature. ERK dimers were detected on nitrocellulose membranes by luminol chemiluminescence kit (Bio Rad ECL, USA) using X-Ray film (Agfa ORTHO CP-GU, cat. PTNAGCPGUM2, Voxel, Argentina). SDS-PAGE blots were developed using the same chemiluminescence kit in a GE Amersham Imager.

Table 1.

Target	Supplier	Carrier solution	Dilution
ERK2	Santa Cruz (SC-1647)	4 % milk in TBS - 0.05 % (v/v) Tween	1:1000
pERK1/2	Cell Signaling (9101)	4 % milk in TBS - 1 % (v/v) Tween	1:2000
ERK1/2	Cell Signaling (9102)		1:2000
Rabbit IgG	Santa Cruz (SC-2357)		1:10000
Mouse IgG	Cell Signaling (7076)		1:15000

Data analysis

Data analyses were conducted using R (version 4.2.2,83; R core team, 2021). Generalized linear models (GLMs) were employed using the glmmTMB package (version 1.1.6; Brooks et al., 2017). For behavioral data (latency to step-through), drug (VEH or DEL) and condition (RE or NR) were used as fixed factors. The model was fitted with a Gamma distribution and log link function. For western blot data, the model was fitted using a Gaussian distribution and identity link function. Repeated measures ANOVA with Time and Treatment as fixed factors was used to analyze the LTP experiment. The goodness-of-fit for each model was evaluated using the DHARMa package (version 0.4.6; Hartig, 2024). Visual inspection of residual plots did not reveal any concerning deviations from normality or homoscedasticity. ANOVA of the models is reported and, when applicable, post-hoc comparisons were performed using the emmeans package (version 1.8.5; Lenth, 2017). All reported p-values were adjusted for multiple comparisons with the Šidak correction method. Two-tailed Pearson coefficients were calculated to determine the correlation between phosphorylation and dimerization at each time point.

Funding

This work was supported by the following grants: Agencia Nacional de Promoción de la Investigación, el Desarrollo Tecnológico y la Innovación (ANPCYT PICT 2016 0295, ANPCYT PICT 2020 01534 and PICT 2015 1199), Consejo Nacional de Investigaciones Científicas y Técnicas (CONICET PIP 2014-2016 No. 11220130100519CO) and Universidad de Buenos Aires (UBACYT 2018-2021 - 20020170100390BA and 2014-2017 - 20020130200283BA), Argentina.

Author Contributions

S.O.R. performed experiments, analyzed data, and contributed to writing parts of the manuscript. C.M. performed behavioral experiments, analyzed data, and reviewed the manuscript. M.C.K., J.M. and M.F.A. performed experiments and reviewed the manuscript. M.V.B. performed experiments and contributed to writing parts of the manuscript. M.M.B contributed to designing the experiments, performed behavioral experiments and interpreted data. A.G.R contributed to data analysis and reviewed the manuscript. F.J.U. & S.O.R. designed and performed electrophysiology experiments in slices, interpreted data. M.F. proposed the original research project, designed experiments and performed biochemical assays, interpreted data, and drafted the manuscript.

Conflicts of Interest

The authors declare no conflicts of interest.

REFERENCES

Acutain MF, Griebler Luft J, Vazquez CA, Popik B, Cercato MC, Epstein A, Salvetti A, Jerusalinsky DA, de Oliveira Alvares L, Baez MV. 2021. Reduced Expression of Hippocampal GluN2A-NMDAR Increases Seizure Susceptibility and Causes Deficits in Contextual Memory. *Front Neurosci* **15**:644100. doi:10.3389/fnins.2021.644100

Afinanisa Q, Cho MK, Seong H-A. 2021. AMPK Localization: A Key to Differential Energy Regulation. *Int J Mol Sci* **22**:10921. doi:10.3390/ijms222010921

Ahn NG. 2009. PORE-ing over ERK substrates. *Nat Struct Mol Biol* **16**:1004–1005. doi:10.1038/nsmb1009-1004

Albert-Gascó H, Ros-Bernal F, Castillo-Gómez E, Olucha-Bordonau F. 2020. MAP/ERK Signaling in Developing Cognitive and Emotional Function and Its Effect on Pathological and Neurodegenerative Processes. *Int J Mol Sci* **21**. doi:10.3390/ijms21124471

Atkins CM, Selcher JC, Petraitis JJ, Trzaskos JM, Sweatt JD. 1998. The MAPK cascade is required for mammalian associative learning. *Nat Neurosci* **1**:602–609. doi:10.1038/2836

Blake MG, Boccia MM, Baratti CM. 2008. Behavioral differences on memory retrieval between two variants of step-through inhibitory avoidance task in mice. *Neurosci Lett* **444**:102–105. doi:10.1016/j.neulet.2008.08.010

Blake MG, Krawczyk MC, Baratti CM, Boccia MM. 2014. Neuropharmacology of memory consolidation and reconsolidation: Insights on central cholinergic mechanisms. *J Physiol Paris*. doi:10.1016/j.jphysparis.2014.04.005

Bliss TV, Collingridge GL. 1993. A synaptic model of memory: long-term potentiation in the hippocampus. *Nature* **361**:31–39. doi:10.1038/361031a0

Bliss TVP, Lømo T. 1973. Long-lasting potentiation of synaptic transmission in the dentate area of the anaesthetized rabbit following stimulation of the perforant path. *J Physiol* **232**:331–356. doi:10.1113/jphysiol.1973.sp010273

Blum S, Moore AN, Adams F, Dash PK. 1999. A mitogen-activated protein kinase cascade in the CA1/CA2 subfield of the dorsal hippocampus is essential for long-term spatial memory. *J Neurosci Off J Soc Neurosci* **19**:3535–3544.

Boccia M, Freudenthal R, Blake M, de la Fuente V, Acosta G, Baratti C, Romano A. 2007. Activation of hippocampal nuclear factor-kappa B by retrieval is required for memory reconsolidation. *J Neurosci Off J Soc Neurosci* **27**:13436–13445. doi:10.1523/JNEUROSCI.4430-07.2007

Boccia MM, Acosta GB, Blake MG, Baratti CM. 2004. Memory consolidation and reconsolidation of an inhibitory avoidance response in mice: effects of i.c.v. injections of hemicholinium-3. *Neuroscience* **124**:735–741. doi:10.1016/j.neuroscience.2004.01.001

Boccia MM, Blake MG, Krawczyk MC, Baratti CM. 2010. Hippocampal α7 nicotinic receptors modulate memory reconsolidation of an inhibitory avoidance task in mice. *Neuroscience* **171**:531–543. doi:10.1016/j.neuroscience.2010.08.027

Boggio EM, Putignano E, Sassoè-Pognetto M, Pizzorusso T, Giustetto M. 2007. Visual stimulation activates ERK in synaptic and somatic compartments of rat cortical neurons with parallel kinetics. *PloS One* **2**:e604. doi:10.1371/journal.pone.0000604

Brooks ME, Kristensen K, Benthem KJ van, Magnusson A, Berg CW, Nielsen A, Skaug HJ, Mächler M, Bolker BM. 2017. glmmTMB Balances Speed and Flexibility Among Packages for Zero-inflated Generalized Linear Mixed Modeling. *R J* **9**:378–400.

Brüggemann Y, Karajannis LS, Stanoev A, Stallaert W, Bastiaens PIH. 2021. Growth factor-dependent ErbB vesicular dynamics couple receptor signaling to spatially and functionally distinct Erk pools. *Sci Signal* **14**:eabd9943. doi:10.1126/scisignal.abd9943

Casar B, Crespo P. 2016. ERK Signals: Scaffolding Scaffolds? *Front Cell Dev Biol* **4**.

Casar B, Pinto A, Crespo P. 2008. Essential role of ERK dimers in the activation of cytoplasmic but not nuclear substrates by ERK-scaffold complexes. *Mol Cell* **31**:708–721. doi:10.1016/j.molcel.2008.07.024

de la Fuente-Vivas D, Cappitelli V, García-Gómez R, Valero-Díaz S, Amato C, Rodriguéz J, Duro-Sánchez S, von Kriegsheim A, Grusch M, Lozano J, Arribas J, Casar B, Crespo P. 2024. ERK1/2 mitogen-activated protein kinase dimerization is essential for the regulation of cell motility. *Mol Oncol*. doi:10.1002/1878-0261.13732

Dudai Y, Eisenberg M. 2004. Rites of passage of the engram: reconsolidation and the lingering consolidation hypothesis. *Neuron* **44**:93–100. doi:10.1016/j.neuron.2004.09.003

Earnest S, Khokhlatchev A, Albanesi JP, Barylko B. 1996. Phosphorylation of dynamin by ERK2 inhibits the dynamin-microtubule interaction. *FEBS Lett* **396**:62–66.

English JD, Sweatt JD. 1997. A requirement for the mitogen-activated protein kinase cascade in hippocampal long term potentiation. *J Biol Chem* **272**:19103–19106. doi:10.1074/jbc.272.31.19103

Feld M, Dimant B, Delorenzi A, Coso O, Romano A. 2005. Phosphorylation of extra-nuclear ERK/MAPK is required for long-term memory consolidation in the crab Chasmagnathus. *Behav Brain Res* **158**:251–261. doi:10.1016/j.bbr.2004.09.005

Feld M, Krawczyk MC, Sol Fustiñana M, Blake MG, Baratti CM, Romano A, Boccia MM. 2014. Decrease of ERK/MAPK overactivation in prefrontal cortex reverses early memory deficit in a mouse model of Alzheimer's disease. *J Alzheimers Dis JAD* **40**:69–82. doi:10.3233/JAD-131076

Formoso K, Lezoualc'h F, Mialet-Perez J. 2020. Role of EPAC1 Signalosomes in Cell Fate: Friends or Foes? *Cells* **9**:1954. doi:10.3390/cells9091954

Fukushima H, Zhang Y, Archbold G, Ishikawa R, Nader K, Kida S. 2014. Enhancement of fear memory by retrieval through reconsolidation. *eLife* **3**:e02736.

Gao C, Frausto SF, Guedea AL, Tronson NC, Jovasevic V, Leaderbrand K, Corcoran KA, Guzmán YF, Swanson GT, Radulovic J. 2011. IQGAP1 regulates NR2A signaling, spine density, and cognitive processes. *J Neurosci Off J Soc Neurosci* **31**:8533–8542. doi:10.1523/JNEUROSCI.1300-11.2011

Gong R, Tang S-J. 2006. Mitogen-activated protein kinase signaling is essential for activity-dependent dendritic protein synthesis. *Neuroreport* **17**:1575–1578. doi:10.1097/01.wnr.0000234742.42818.ff

Hartig F. 2024. DHARMa: residual diagnostics for hierarchical (multi-level/mixed) regression models. *DHARMa*. http://florianhartig.github.io/DHARMa/

Herrero A, Pinto A, Colón-Bolea P, Casar B, Jones M, Agudo-Ibáñez L, Vidal R, Tenbaum SP, Nuciforo P, Valdizán EM, Horvath Z, Orfi L, Pineda-Lucena A, Bony E, Keri G, Rivas G, Pazos A, Gozalbes R, Palmer HG, Hurlstone A, Crespo P. 2015. Small Molecule Inhibition of ERK Dimerization Prevents Tumorigenesis by RAS-ERK Pathway Oncogenes. *Cancer Cell* **28**:170–182. doi:10.1016/j.ccell.2015.07.001

Impey S, Obrietan K, Wong ST, Poser S, Yano S, Wayman G, Deloulme JC, Chan G, Storm DR. 1998. Cross talk between ERK and PKA is required for Ca2+ stimulation of CREB-dependent transcription and ERK nuclear translocation. *Neuron* **21**:869–883. doi:10.1016/s0896-6273(00)80602-9

Kaech S, Banker G. 2006. Culturing hippocampal neurons. *Nat Protoc* **1**:2406–2415. doi:10.1038/nprot.2006.356

Kelleher RJ 3rd, Govindarajan A, Jung H-Y, Kang H, Tonegawa S. 2004. Translational control by MAPK signaling in long-term synaptic plasticity and memory. *Cell* **116**:467–479.

Khokhlatchev AV, Canagarajah B, Wilsbacher J, Robinson M, Atkinson M, Goldsmith E, Cobb MH. 1998. Phosphorylation of the MAP kinase ERK2 promotes its homodimerization and nuclear translocation. *Cell* **93**:605–615. doi:10.1016/s0092-8674(00)81189-7

Kneussel M, Wagner W. 2013. Myosin motors at neuronal synapses: drivers of membrane transport and actin dynamics. *Nat Rev Neurosci* **14**:233–247. doi:10.1038/nrn3445

Krawczyk MC, Blake MG, Baratti CM, Romano A, Boccia MM, Feld M. 2015. Memory reconsolidation of an inhibitory avoidance task in mice involves cytosolic ERK2 bidirectional modulation. *Neuroscience* **294**:227–237. doi:10.1016/j.neuroscience.2015.03.019

Krawczyk MC, Millan J, Blake MG, Boccia MM. 2021. Role of prediction error and the cholinergic system on memory reconsolidation processes in mice. *Neurobiol Learn Mem* **185**:107534. doi:10.1016/j.nlm.2021.107534

Krawczyk MC, Millan J, Blake MG, Feld M, Boccia MM. 2019. Relevance of ERK1/2 Post-retrieval Participation on Memory Processes: Insights in Their Particular Role on

Reconsolidation and Persistence of Memories. *Front Mol Neurosci* **12**:95. doi:10.3389/fnmol.2019.00095

Krawczyk MC, Navarro N, Blake MG, Romano A, Feld M, Boccia MM. 2016. Reconsolidation-induced memory persistence: Participation of late phase hippocampal ERK activation. *Neurobiol Learn Mem* **133**:79–88. doi:10.1016/j.nlm.2016.06.013

Lavoie H, Gagnon J, Therrien M. 2020. ERK signalling: a master regulator of cell behaviour, life and fate. *Nat Rev Mol Cell Biol* **21**:607–632. doi:10.1038/s41580-020-0255-7

Lenth RV. 2017. emmeans: Estimated Marginal Means, aka Least-Squares Means. doi:10.32614/CRAN.package.emmeans

Marshall CJ. 1995. Specificity of receptor tyrosine kinase signaling: transient versus sustained extracellular signal-regulated kinase activation. *Cell* **80**:179–185. doi:10.1016/0092-8674(95)90401-8

Martin KC, Michael D, Rose JC, Barad M, Casadio A, Zhu H, Kandel ER. 1997. MAP kinase translocates into the nucleus of the presynaptic cell and is required for long-term facilitation in Aplysia. *Neuron* **18**:899–912.

Miningou N, Blackwell KT. 2020. The road to ERK activation: Do neurons take alternate routes? *Cell Signal* **68**:109541. doi:10.1016/j.cellsig.2020.109541

Nader K, Schafe GE, LeDoux JE. 2000. The labile nature of consolidation theory. *Nat Rev Neurosci* **1**:216–219. doi:10.1038/35044580

Nguyen TT, Scimeca JC, Filloux C, Peraldi P, Carpentier JL, Van Obberghen E. 1993. Co-regulation of the mitogen-activated protein kinase, extracellular signal-regulated kinase 1, and the 90-kDa ribosomal S6 kinase in PC12 cells. Distinct effects of the neurotrophic factor, nerve growth factor, and the mitogenic factor, epidermal growth factor. *J Biol Chem* **268**:9803–9810. doi:10.1016/S0021-9258(18)98418-8

Ojea Ramos S, Feld M, Fustiñana MS. 2022. Contributions of extracellular-signal regulated kinase 1/2 activity to the memory trace. *Front Mol Neurosci* **15**. doi:10.3389/fnmol.2022.988790

Paxinos G, Franklin KBJ. 2019. The Mouse Brain in Stereotaxic Coordinates, 5th ed. Academic Press.

Pinto A, Crespo P. 2010. Analysis of ERKs' dimerization by electrophoresis. *Methods Mol Biol Clifton NJ* **661**:335–342. doi:10.1007/978-1-60761-795-2_20

Pirbhoy PS, Farris S, Steward O. 2017. Synaptically driven phosphorylation of ribosomal protein S6 is differentially regulated at active synapses versus dendrites and cell bodies by MAPK and PI3K/mTOR signaling pathways. *Learn Mem Cold Spring Harb N* **24**:341–357. doi:10.1101/lm.044974.117

R core team. 2021. R: The R Project for Statistical Computing. https://www.r-project.org/

Rivero-Echeto MC, Perissinotti PP, González-Inchauspe C, Kargieman L, Bisagno V, Urbano FJ. 2021. Simultaneous administration of cocaine and caffeine dysregulates HCN and T-type channels. *Psychopharmacology (Berl)* **238**:787–810. doi:10.1007/s00213-020-05731-5

Romano R, Bucci C. 2020. Role of EGFR in the Nervous System. *Cells* **9**:1887. doi:10.3390/cells9081887

Salles A, Boccia M, Blake M, Corbi N, Passananti C, Baratti CM, Romano A, Freudenthal R. 2015. Hippocampal dynamics of synaptic NF-kappa B during inhibitory avoidance long-term memory consolidation in mice. *Neuroscience* **291**:70–80. doi:10.1016/j.neuroscience.2015.01.063

Sara SJ. 2000. Retrieval and reconsolidation: toward a neurobiology of remembering. *Learn Mem Cold Spring Harb N* **7**:73–84.

Schafe GE, Atkins CM, Swank MW, Bauer EP, Sweatt JD, LeDoux JE. 2000. Activation of ERK/MAP kinase in the amygdala is required for memory consolidation of pavlovian fear conditioning. *J Neurosci Off J Soc Neurosci* **20**:8177–8187. doi:10.1523/JNEUROSCI.20-21-08177.2000

Schrader LA, Birnbaum SG, Nadin BM, Ren Y, Bui D, Anderson AE, Sweatt JD. 2006. ERK/MAPK regulates the Kv4.2 potassium channel by direct phosphorylation of the

pore-forming subunit. *Am J Physiol Cell Physiol* **290**:C852-861. doi:10.1152/ajpcell.00358.2005

Selcher JC, Weeber EJ, Christian J, Nekrasova T, Landreth GE, Sweatt JD. 2003. A Role for ERK MAP Kinase in Physiologic Temporal Integration in Hippocampal Area CA1. *Learn Mem* **10**:26–39. doi:10.1101/lm.51103

Swanger SA, He YA, Richter JD, Bassell GJ. 2013. Dendritic GluN2A Synthesis Mediates Activity-Induced NMDA Receptor Insertion. *J Neurosci* **33**:8898–8908. doi:10.1523/JNEUROSCI.0289-13.2013

Traverse S, Gomez N, Paterson H, Marshall C, Cohen P. 1992. Sustained activation of the mitogen-activated protein (MAP) kinase cascade may be required for differentiation of PC12 cells. Comparison of the effects of nerve growth factor and epidermal growth factor. *Biochem J* **288 (Pt 2)**:351–355. doi:10.1042/bj2880351

Walz R, Roesler R, Barros DM, de Souza MM, Rodrigues C, Sant'Anna MK, Quevedo J, Choi HK, Neto WP, DeDavid e Silva TL, Medina JH, Izquierdo I. 1999. Effects of post-training infusions of a mitogen-activated protein kinase kinase inhibitor into the hippocampus or entorhinal cortex on short- and long-term retention of inhibitory avoidance. *Behav Pharmacol* **10**:723–730.

Xing C, Imagawa W. 1999. Altered MAP kinase (ERK1,2) regulation in primary cultures of mammary tumor cells: elevated basal activity and sustained response to EGF. *Carcinogenesis* **20**:1201–1208. doi:10.1093/carcin/20.7.1201

Zaballos MA, Acuña-Ruiz A, Morante M, Riesco-Eizaguirre G, Crespo P, Santisteban P. 2022. Inhibiting ERK dimerization ameliorates BRAF-driven anaplastic thyroid cancer. *Cell Mol Life Sci CMLS* **79**:504. doi:10.1007/s00018-022-04530-9

Zamorano C, Fernández-Albert J, Storm DR, Carné X, Sindreu C. 2018. Memory Retrieval Re-Activates Erk1/2 Signaling in the Same Set of CA1 Neurons Recruited During Conditioning. *Neuroscience* **370**:101–111. doi:10.1016/j.neuroscience.2017.03.034